

Copyright WILEY-VCH Verlag GmbH & Co. KGaA, 69469 Weinheim, Germany, 2016.

## Supporting Information

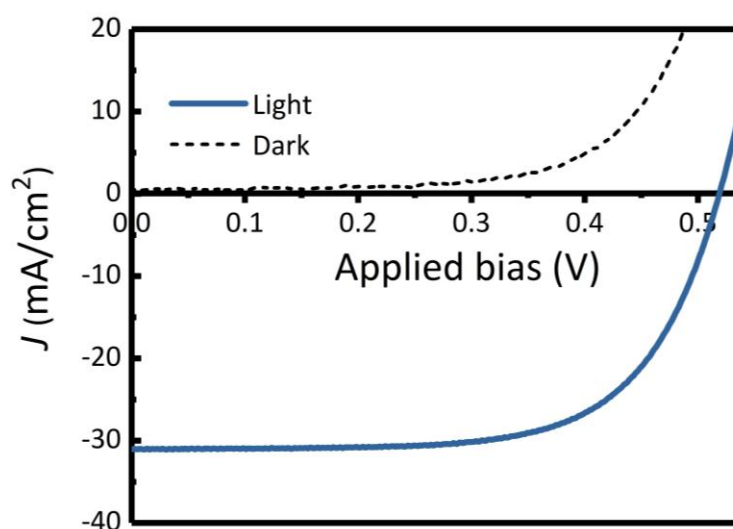
### **A High Efficiency Si Photoanode Protected by Few-Layer MoSe<sub>2</sub>**

*Srinivas Vanka, Yongjie Wang, Pegah Ghamari, Sheng Chu, Ayush Pandey, Pallab Bhattacharya, Ishiang Shih, and Zetian Mi\**

S. Vanka, Y. Wang, A. Pandey, Prof. P. Bhattacharya and Prof. Z. Mi  
Department of Electrical Engineering and Computer Science, University of Michigan, Ann Arbor,  
1301 Beal Avenue, Ann Arbor, MI 48109, USA

S. Vanka, Dr. S. Chu, P. Ghamari, Prof. I. Shih and Prof. Z. Mi  
Department of Electrical and Computer Engineering, McGill University, 3480 University Street,  
Montreal, Quebec H3A 0E9, Canada

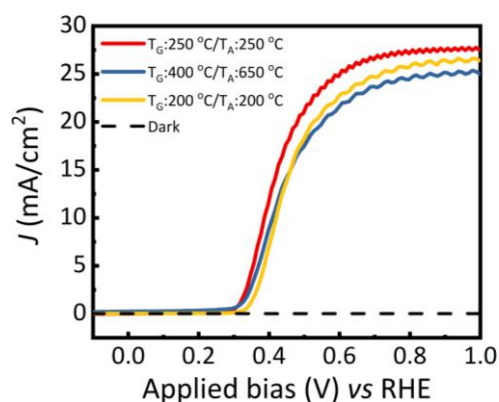
E-mail: ztmi@umich.edu

Supporting Information Section 1: Fabrication of  $p^+n$  Si Wafer

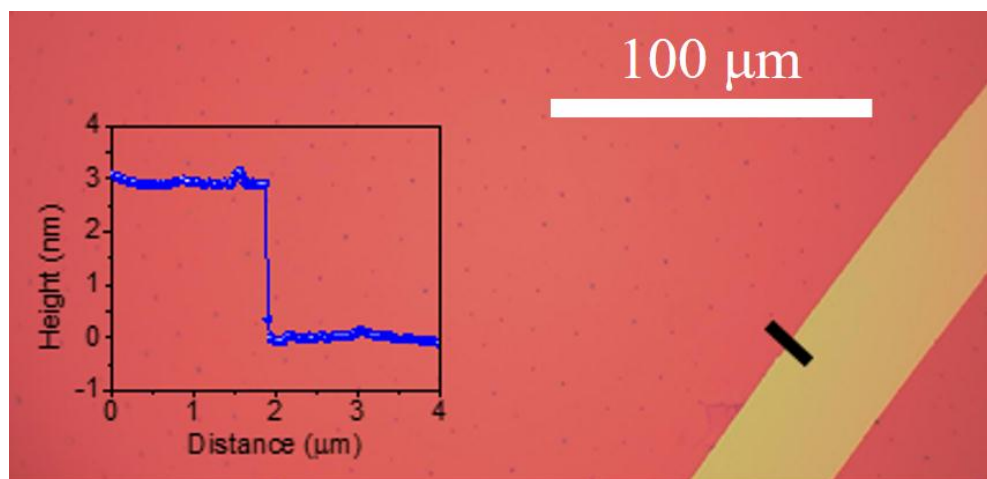
**Figure S1.**  $J$ - $V$  characteristics of  $p^+n$  Si solar cell under AM1.5G one sun illumination 100  $\text{mW}/\text{cm}^2$  (dark blue curve) and dark condition (black dashed curve). The current density shown in the figure is limited by the reflection of incident light <sup>[1, 2]</sup>.

## Supporting Information Section 2: Effect of MoSe<sub>2</sub> Growth Conditions on the PEC Performance

To study the effect of growth temperature ( $T_G$ ) and annealing temperature ( $T_A$ ) in the two step MBE growth (see main text), samples with different growth and annealing temperature combinations were grown by keeping the same thickness of 3 nm for the MoSe<sub>2</sub> film. Shown in Figure S2, it can be observed that the best PEC performing sample, in terms of on-set voltage and photocurrent density, is with growth temperature of 250 °C and annealing temperature of 250 °C. The sample with growth temperature of 400 °C showed lower photocurrent density and the sample with growth temperature 200 °C produced a lower on-set potential compared to the sample with growth temperature 250 °C.



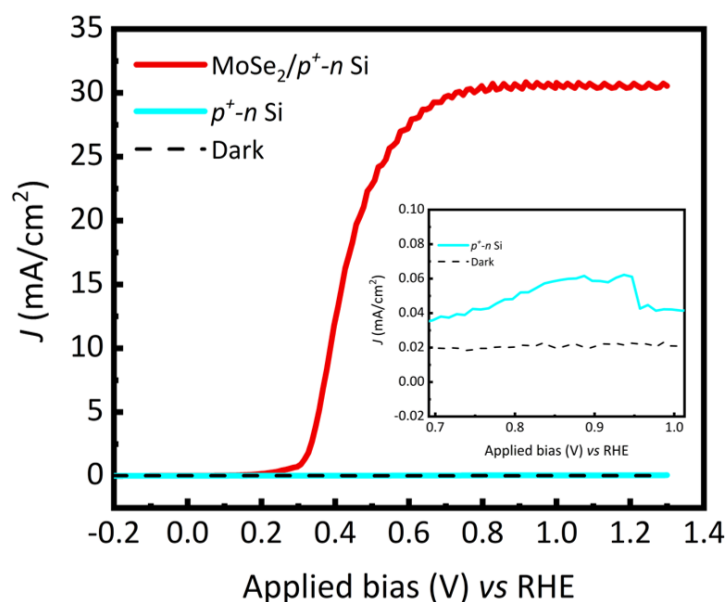
**Figure S2.** *J-V* characteristics of MoSe<sub>2</sub> thin films (~3 nm thick) on  $p^+ - n$  Si wafer with different growth combinations of growth temperature ( $T_G$ ) and annealing temperature ( $T_A$ ) under AM1.5G one sun illumination 100 mW/cm<sup>2</sup> and dark condition (black dashed curve) in 1M HBr.  $T_G$ : 250 °C/  $T_A$ : 250 °C (red curve),  $T_G$ : 400 °C/  $T_A$ : 650 °C (blue curve), and  $T_G$ : 200 °C/  $T_A$ : 200 °C (yellow curve).

Supplementary Information Section 3: Structural Characterization of MoSe<sub>2</sub>

**Figure S3.** Optical microscopy image of MoSe<sub>2</sub> with a thickness of ~3 nm. The atomic force microscopy measurement performed near the black bar region is shown in the inset.

**Supporting Information Section 4: PEC Performance of  $p^+ - n$  Si Photoanode**

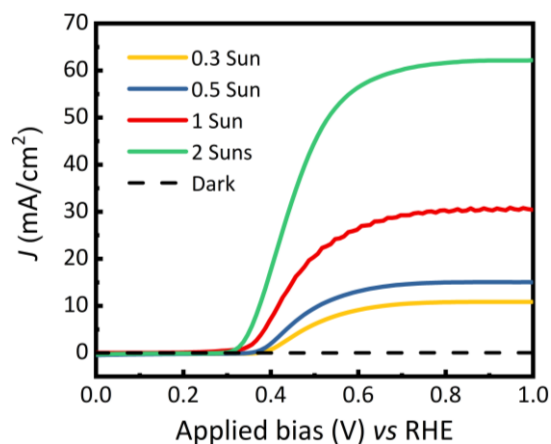
J-V curves (see Figure S4) show that the photocurrent density for  $p^+ - n$  Si photoanode (light blue curve) without MoSe<sub>2</sub> protection layer is almost negligible, compared to MoSe<sub>2</sub>/ $p^+ - n$  Si photoanode (red curve). This can be attributed to the fact that unprotected Si surface is highly prone to oxidation<sup>[3]</sup> in acidic solution, which results in extremely low current density and poor stability. As shown by the red curve in Figure S4, the sample with MoSe<sub>2</sub> protection layer exhibited a high saturated photocurrent density of ~30 mA/cm<sup>2</sup>.



**Figure S4.** LSV curves showing a comparison between with (red curve) and without (light blue curve) MoSe<sub>2</sub> thin film on  $p^+ - n$  Si photoanode in 1M HBr solution under the illumination of AM1.5G one sun (100 mW/cm<sup>2</sup>) and dark condition (black dashed curve). Inset shows the comparison between  $p^+ - n$  Si solar cell under AM1.5G one sun illumination (light blue curve) and dark condition (dotted black curve) in the potential range of 0.7-1 V vs RHE.

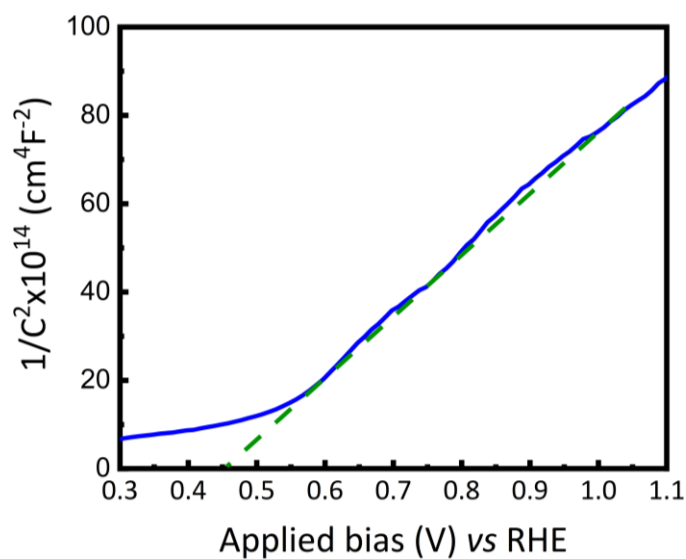
**Supporting Information Section 5: PEC Performance of MoSe<sub>2</sub>/p<sup>+</sup>-n Si Photoanode**

The saturated photocurrent density of  $\sim 30$  mA/cm<sup>2</sup> is close to the maximum theoretical current density for c-Si, considering surface reflection loss of the incident light. In fact, the measured photocurrent density is nearly identical to the  $J_{sc}$  of the Si solar cell shown in Figure S1, which suggests that photo-generated holes in Si can effectively tunnel through the thin MoSe<sub>2</sub> protection layer and participate in oxidation reaction. We have further tested the PEC performance by varying the light intensity. Shown in Figure S5 are the measurements performed under different light illuminations: 0.3 Sun, 0.5 Sun, 1 Sun and 2 Suns, with the saturated photocurrent being 11 mA/cm<sup>2</sup>, 15 mA/cm<sup>2</sup>, 30 mA/cm<sup>2</sup> and 60 mA/cm<sup>2</sup>, respectively. The photocurrent density scales linearly with the light intensity. The light-limited photocurrent density values also agree well with previous reports [4-8].

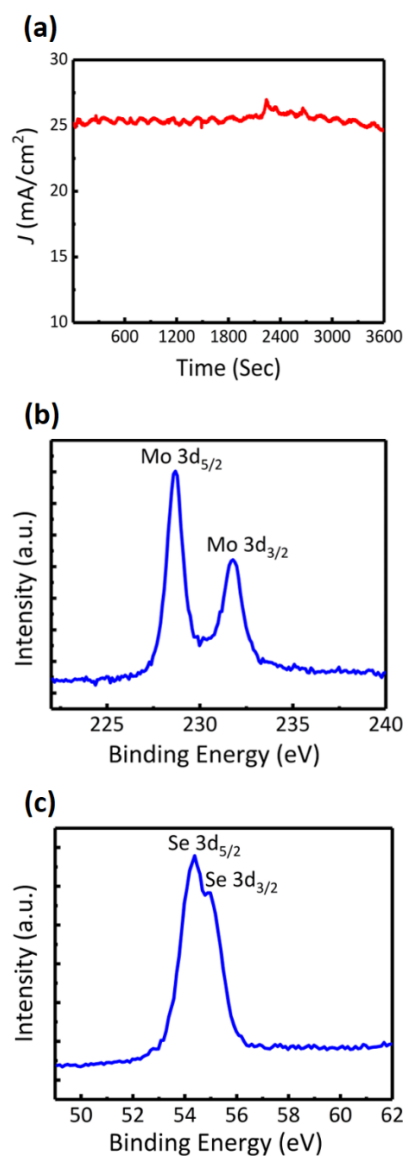


**Figure S5.**  $J$ - $V$  characteristics of MoSe<sub>2</sub>/p<sup>+</sup>-n Si photoanode under different illumination conditions in 1 M HBr under various illumination intensities: 0.3 Sun (yellow curve), 0.5 Sun (blue curve), 1 Sun (red curve) and 2 Suns (green curve) and dark condition (black dashed curve).

Supporting Information Section 6: Mott-Schottky Characteristics of MoSe<sub>2</sub>/p<sup>+</sup>-n Si  
Photoanode



**Figure S6.** Mott-Schottky characteristics of MoSe<sub>2</sub>/p<sup>+</sup>-n Si photoanode measured at 1 KHz under dark condition (blue curve) in 1M HBr and the extrapolated linear fit (green dashed line) intercepts the x-axis at 0.46 V vs RHE. From the Figure S6, the positive slope indicates *n*-type behaviour which is characteristic of photoanode. The  $V_{fb}$  from this analysis is ~0.46 V vs RHE which is close to the value reported in the main text using OCP analysis.

Supporting Information Section 7: Stability of MoSe<sub>2</sub>/p<sup>+</sup>-n Si photoanode

**Figure S7.** (a) Chronoamperometry study for MoSe<sub>2</sub>/p<sup>+</sup>-n Si photoanode shows stable photocurrent density of ~ 26 mA/cm<sup>2</sup> at 0.6 V vs RHE for 1 hr. XPS measurements after 1 hr chronoamperometry stability test for (b) Mo and (c) Se, showing Mo:Se ratio of ~1:2.

**Supporting Information Section 8: On the Hole Injection Efficiency**

The light-limited current density for MoSe<sub>2</sub>/p<sup>+</sup>-n Si solar cell photoanode is 30 mA/cm<sup>2</sup>. Based on this observation, we have further calculated the hole injection efficiency for photoanodes with different thicknesses of MoSe<sub>2</sub>. As seen from Figure S8, at relatively low bias ~0.5-0.6 V vs RHE the hole injection efficiency is ≥ 80% for MoSe<sub>2</sub> thicknesses of 3 nm and 5 nm. The shaded region in Figure S8 indicates hole injection efficiency >80%. The achievement of very high hole injection efficiency at a relatively low biasing voltage suggests the efficient tunneling of photogenerated holes from Si to solution through the MoSe<sub>2</sub> protection layer.

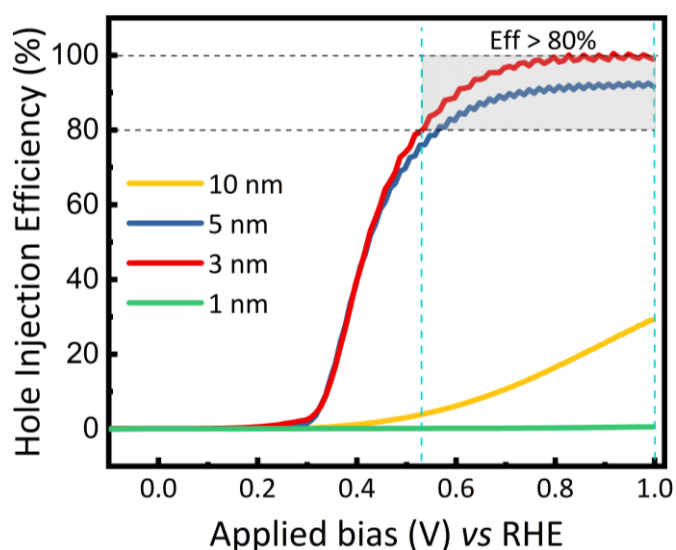


**Figure S8.** Hole injection efficiency for MoSe<sub>2</sub>/p<sup>+</sup>-n Si photoanodes with different MoSe<sub>2</sub> thicknesses under AM 1.5G one sun illumination in 1 M HBr. The shaded region indicates hole injection efficiency between >80%.

## References

1. L. A. Osminkina, K. A. Gonchar, V. S. Marshov, K. V. Bunkov, D. V. Petrov, L. A. Golovan, F. Talkenberg, V. A. Sivakov, V. Y. Timoshenko, *Nanoscale Research Letters* **2012**, *7*, (1), 524.
2. R. Santbergen, *Optical absorption factor of solar cells for PVT Systems*. Eindhoven University Press: 2008.
3. A. Q. Contractor, J. O. M. Bockris, *Electrochim. Acta* **1984**, *29*, (10), 1427-1434.
4. S. Hu, M. R. Shaner, J. A. Beardslee, M. Lichterman, B. S. Brunshwig, N. S. Lewis, *Science* **2014**, *344*, (6187), 1005-1009.
5. X. Yu, P. Yang, S. Chen, M. Zhang, G. Shi, *Adv. Energ. Mater.* **2017**, *7*, (6), 1601805.
6. J. Yang, K. Walczak, E. Anzenberg, F. M. Toma, G. Yuan, J. Beeman, A. Schwartzberg, Y. Lin, M. Hettick, A. Javey, J. W. Ager, J. Yano, H. Frei, I. D. Sharp, *J. Am. Chem. Soc.* **2014**, *136*, (17), 6191-4.
7. K. Sun, M. T. McDowell, A. C. Nielander, S. Hu, M. R. Shaner, F. Yang, B. S. Brunshwig, N. S. Lewis, *J. Phys. Chem. Lett.* **2015**, *6*, (4), 592-8.
8. X. H. Zhou, R. Liu, K. Sun, D. Friedrich, M. T. McDowell, F. Yang, S. T. Omelchenko, F. H. Saadi, A. C. Nielander, S. Yalamanchili, K. M. Papadantonakis, B. S. Brunshwig, N. S. Lewis, *Energ. Environ. Sci.* **2015**, *8*, (9), 2644-2649.